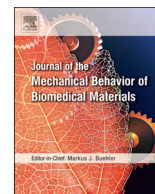




Contents lists available at ScienceDirect

Journal of the Mechanical Behavior of Biomedical Materials

journal homepage: www.elsevier.com/locate/jmbbm

Mechanical alterations of the bone-cartilage unit in a rabbit model of early osteoarthritis

Sarah Pragnère^a, Caroline Boulocher^b, Ophélie Pollet^a, Catherine Bosser^a, Aurélie Levillain^a, Magali Cruel^a, Thierry Hoc^{a,*}

^a LTDS UMR 5513, Ecole Centrale de Lyon, 36 Avenue Guy de Collongue, 69134 Ecully Cedex, France

^b VetAgro Sup, 1 Avenue Bourgelat, 69280 Marcy-l'Étoile, France

ARTICLE INFO

Keywords:

Cartilage mechanics
Bone mechanics
Osteoarthritis
Biphoton imaging
Mineralization
Nanoindentation
Hyaline cartilage
Calcified cartilage
Subchondral bone

ABSTRACT

Objective: The purpose of this study was to assess mechanical properties along with microstructural modifications of the hyaline cartilage (HC), calcified cartilage (CC) and cortical plate (Ct.Pt), in an anterior cruciate ligament transection (ACLT) model.

Medial femoral condyles of six healthy rabbits (control group) and of six ACLT rabbits 6 weeks after OA induction were explanted. The zone of interest (ZOI) for all experiments was defined as the weight bearing areas of the samples. Biomechanical properties were measured using nanoindentation and morphological changes were evaluated using biphotonic confocal microscopy (BCM).

Results: All rabbits of the ACLT group displayed early PTOA. The results indicate an overall decrease in the mechanical properties of the HC, CC and Ct.Pt in the ACLT group. The average equilibrium modulus and elastic fraction of the HC decreased by 42% and 35%, respectively, compared with control group. The elastic moduli of the CC and Ct.Pt decreased by 37% and 16%, respectively, compared with control group. A stiffness gradient between CC and Ct.Pt appeared in the ACLT group. The irregularity of the cement line, quantified by its tortuosity in BCM images, was accentuated in the ACLT group compared with the control group.

Conclusions: In the ACLT model, weight-bearing stress was modified in the ZOI. This disruption of the stress pattern induced alterations of the tissues composing the bone-cartilage unit. In term of mechanical properties, all tissues exhibited changes. The most affected tissue was the most superficial: hyaline cartilage displayed the strongest relative decrease (42%) followed by calcified cartilage (37%) and cortical plate was slightly modified (16%). This supports the hypotheses that PTOA initiates in the hyaline cartilage.

1. Introduction

Osteoarthritis (OA) is involved in the degradation of the whole joint, including articular cartilage and subchondral bone, composing together the bone-cartilage unit (BCU) (Lories and Luyten, 2011). Articular cartilage is a complex viscous-elastic tissue made of several layers, tethered to the subchondral bone by the osteochondral junction. This osteochondral junction lies beneath the tidemark, which is a line that delineates the bottom of the hyaline articular cartilage *i.e.* between the uncalcified (hyaline) and calcified cartilage. The osteochondral junction includes the mineralised tissues, *i.e.* calcified cartilage (CC) and the subchondral cortical plate (Ct.Pt), which are separated from each other by the cement line (Ferguson and Paietta, 2013). These two mineralised tissues are tightly anchored through a highly interdigitated interface and are linked by some collagen fibres that cross the cement line

(Mansfield and Peter Winlove, 2012). Whether the changes in the osteochondral junction occurring in OA are a cause or a consequence of hyaline cartilage damage is still debated (Burr and Gallant, 2012).

Mechanical modification of loads by increased focal stress or excess overall load are factors that lead to OA (Felson, 2013). Because one of the major roles of both the articular cartilage and osteochondral junction is to absorb and transmit forces across the whole joint, any modification of these tightly linked tissues plays an important role in OA onset and progression (Burr, 2004). Calcified cartilage acts as an interface between the compliant hyaline cartilage and the stiffer cortical plate, which permits load transfer while preventing large cartilage deformation (Oegema *et al.*, 1997). In particular, it is thought to transform shear stress into compression (Norrdin *et al.*, 1999; Thambyah and Broom, 2009). In addition, its low permeability limits the diffusion of molecules from bone towards the hyaline cartilage and therefore

* Correspondence to: LTDS Batiment G8, Ecole Centrale de Lyon, 36 Av Guy de Collongue, 69134 Ecully Cedex France.
E-mail address: Thierry.hoc@ec-lyon.fr (T. Hoc).

represents a barrier for hyaline cartilage mineralization (Arkill and Winlove, 2008). Only a few studies have focused on the mechanical properties of each individual component of the bone-cartilage unit (Ferguson et al., 2003; Richard et al., 2013). Besides, to our knowledge, no studies have assessed the alterations of the mechanical properties of hyaline cartilage along with the osteochondral junction in a rabbit model of OA.

Recently, several studies have focused on changes in the subchondral trabecular bone in both human (Podsiadlo et al., 2008; Eckstein et al., 2009; Tomanik et al., 2016) and animal models (Bouchgaa et al., 2009; Florea et al., 2015; Kuroki et al., 2011) and have shown that cortical bone plate remodelling increases during OA establishment (Rieger et al., 2017). In the very early stages of OA, cortical plate thickness decreases. In later stages of OA, sclerosis is observed and the subchondral bone mineral content diminishes, which results in a weakening of the mechanical properties at the tissue scale (Li and Aspdén, 1997). However, the evolution of calcified cartilage thickness remains unclear, especially in early OA (Burr and Gallant, 2012). Indeed, calcified cartilage thickness evolution depends both on its progression into hyaline articular cartilage and on the progression of bone into the calcified cartilage. Furthermore, in the calcified cartilage, increased vascular invasion due to angiogenic activity has been observed in all stages of OA (Burr and Gallant, 2012; Saito et al., 2012; Suri et al., 2007). Nonetheless, osteochondral junction alterations during OA remains understudied from a mechanical point of view.

Animal models provide useful information to study the mechanisms involved in OA. Notably, they allow temporal monitoring of OA changes in the early stages. Especially, OA can be induced surgically, which mimics post traumatic OA (PTOA) that occurs in humans and results in altered load bearing (Lampropoulou-Adamidou et al., 2014; Bendele, 2001). In the present study, a model of anterior cruciate ligament transection (ACLT) in rabbit knees was chosen because it is a well-established model of PTOA (Rieger et al., 2017; Saito et al., 2012; Laverty et al., 2010; Batiste et al., 2004; Sah et al., 1997) that results in true instability-induced OA lesions (Mansour et al., 1997; Kuyinu et al., 2016; McCoy, 2015). These instabilities are assumed to increase the risk of developing OA in human patients (Bonnin et al., 1996; Louboutin et al., 2009), therefore understanding the course of PTOA is a major health issue.

The aim of the present study was to assess the mechanical properties of hyaline cartilage, calcified cartilage and cortical plate in an ACLT model. These mechanical modifications were correlated to changes in the morphology of the osteochondral junction using biphotonic confocal microscopy.

2. Materials and methods

2.1. Animal model

All of the experiments and procedures involving animals were approved by the local Ethics Committee (ComEth Anses/ENVA/UPEC number 16) and were performed in full accordance with European legislation. Twelve healthy adult male New Zealand White rabbits (six months of age, 3.8 kg in weight on average) free of degenerative joint disease were obtained from a licensed vendor (EUROLAP, Gosné, France). After two weeks in acclimatization and quarantine, two groups were constituted randomly: a control group (healthy, not operated) ($n = 6$) and an operated group ($n = 6$). In the operated group, experimental OA was surgically induced by ACLT and performed by a trained veterinary surgeon in the right knee (stifle) of the six rabbits. The operated limb was not immobilized postoperatively, and the rabbits were allowed to move freely in their individual cages immediately after surgery. The six rabbits of the control (healthy) group were left unoperated. After a six-week observation period, the rabbits from the control and ACLT groups were euthanized. Both knees were explanted from each animal, carefully dissected, and the menisci were detached.

Meniscus and cartilage degradations, as well as osteophyte production, were graded in right knees (healthy control ($n = 6$), and operated ($n = 6$)) using a macroscopic grading system developed by Laverty et al. (2010).

2.2. Hyaline cartilage mechanical testing

Immediately after removal, right femurs from both control ($n = 6$) and ACLT ($n = 6$) groups were sawed above the distal epiphysis of femur and stored at -20°C until they were used in experiments. The femoral condyles were thawed at room temperature for a couple of hours and then sawed along the longitudinal axis of the femur to separate the medial femoral condyles (MFC) from their lateral counterpart. Indentation-relaxation tests were performed following previously published protocol (Levillain et al., 2017) on each sample surrounded by a physiological saline solution at ambient temperature using a commercial nanoindenter (Agilent Nanoindenter G200, ScienTec, Les Ulis, France). The indenter was a spherical sapphire tip with a radius of curvature of 0.479 mm. The subchondral part of the condyle was glued onto a support. The zone of interest (ZOI) was defined at the load bearing area of the femoral medial condyles as previously described by Vaseenon et al. (2011) (Fig. 1-B). Indentation tests were then conducted on 3 locations in the direction of physiological loading and repeated three times. As classically performed in nanoindentation, a rubber reference material was indented before each series of tests to calibrate the device. A constant displacement rate of $5\ \mu\text{m s}^{-1}$ and a penetration of $40\ \mu\text{m}$ were imposed. The indenter displacement was then maintained for 400 s until equilibrium was reached. Unloading was carried out at $0.05\ \mu\text{m s}^{-1}$.

Instantaneous (E_{ins}), equilibrium (E_{eq}) elastic moduli and elastic fraction ($f = E_{\text{eq}}/E_{\text{ins}}$) were then determined from the resultant force-time data using the viscoelastic model previously published by Levillain et al. (2017) with four branches. The elastic fraction describes the elastic/viscous behaviour of the material ($f = 1$ corresponds to a perfectly elastic material, whereas $f = 0$ corresponds to a perfectly viscous material). The fit of the experimental data obtained with this model is displayed in Fig. 2.

2.3. Calcified cartilage and cortical plate mechanical properties

For each sample ($n = 12$), sagittal sections in the centre of the MFC that were 3 mm thick were prepared as follow. The samples were ground on sand paper (#1200) to obtain planoparallel surfaces then polished using a 1- μm diamond powder and rinsed in an ultrasonication bath. Images taken under an optical microscope were assembled to visualize the entire surface of the MFC (Fig. 1-C).

Nanoindentation tests were performed following published protocol (Imbert et al., 2014) using a commercial nanoindenter (Agilent Nanoindenter G200, ScienTec, Les Ulis, France) to assess tissue mechanical properties (Vaseenon et al., 2011). Fused silica was used for calibration of the Berkovich diamond tip contact surface. The location of each indent was set manually in line with a regular spacing of approximately $100\ \mu\text{m}$, in the area under the hyaline cartilage previously measured. Eleven points were defined in the ZOI of the condyles for the Ct, Pt and the CC of each sample. To ensure that the points fell in the CC, they were placed approximately $30\ \mu\text{m}$ away from the tidemark.

A constant strain rate of $0.05\ \text{s}^{-1}$ and a maximum depth of 2000 nm were imposed. The Continuous Stiffness Measurement (CSM) method allowed for a determination of Young's modulus as a function of the displacement into the surface. The Oliver and Pharr's method (Oliver and Pharr, 1992) was used for this study. The material was assumed to be linear, elastic and isotropic (Zysset et al., 1999). The Poisson ratio was assumed to be 0.3 for both the Ct/Pt and the CC (Stender et al., 2017). Young's modulus for each indentation point was averaged on the plateau between 600 and 800 nm.

Download English Version:

<https://daneshyari.com/en/article/7206988>

Download Persian Version:

<https://daneshyari.com/article/7206988>

[Daneshyari.com](https://daneshyari.com)